OXFORD

Human Molecular Genetics, 2016, Vol. 25, No. 22 4856–4869

doi: 10.1093/hmg/ddw309
Advance Access Publication Date: 5 September 2016
Original Article

ORIGINAL ARTICLE

Influence of prenatal EGCG treatment and *Dyrk1a* dosage reduction on craniofacial features associated with Down syndrome

Samantha D. McElyea[1], John M. Starbuck[2,3], Danika M. Tumbleson-Brink[1], Emily Harrington[1], Joshua D. Blazek[1], Ahmed Ghoneima[2], Katherine Kula[2] and Randall J. Roper[1,*]

[1]Department of Biology, Indiana University-Purdue University Indianapolis, 723 W. Michigan Street, SL306, Indianapolis, IN 46202, USA, [2]Department of Orthodontics and Facial Genetics, Indiana University School of Dentistry, 1121 W. Michigan Street, DS 250B, Indianapolis, IN 46202, USA and [3]Department of Anthropology, University of Central Florida, 4000 Central Florida Blvd., Howard Phillips Hall, Room 309F, Orlando, FL 32816, USA

*To whom correspondence should be addressed. Tel: +317 2748131; Fax: +317 2742846; Email: rjroper@iupui.edu

Abstract

Trisomy 21 (Ts21) affects craniofacial precursors in individuals with Down syndrome (DS). The resultant craniofacial features in all individuals with Ts21 may significantly affect breathing, eating and speaking. Using mouse models of DS, we have traced the origin of DS-associated craniofacial abnormalities to deficiencies in neural crest cell (NCC) craniofacial precursors early in development. Hypothetically, three copies of *Dyrk1a* (dual-specificity tyrosine-(Y)-phosphorylation regulated kinase 1A), a trisomic gene found in most humans with DS and mouse models of DS, may significantly affect craniofacial structure. We hypothesized that we could improve DS-related craniofacial abnormalities in mouse models using a Dyrk1a inhibitor or by normalizing *Dyrk1a* gene dosage. *In vitro* and *in vivo* treatment with Epigallocatechin-3-gallate (EGCG), a Dyrk1a inhibitor, modulated trisomic NCC deficiencies at embryonic time points. Furthermore, prenatal EGCG treatment normalized some craniofacial phenotypes, including cranial vault in adult Ts65Dn mice. Normalization of *Dyrk1a* copy number in an otherwise trisomic Ts65Dn mice normalized many dimensions of the cranial vault, but did not correct all craniofacial anatomy. These data underscore the complexity of the gene–phenotype relationship in trisomy and suggest that changes in *Dyrk1a* expression play an important role in morphogenesis and growth of the cranial vault. These results suggest that a temporally specific prenatal therapy may be an effective way to ameliorate some craniofacial anatomical changes associated with DS.

Introduction

Down syndrome (DS, OMIM 190685) affects 140 of 100 000 live births, and all humans with DS exhibit dysmorphic craniofacial phenotypes and impaired cognition. During prenatal morphogenesis and growth, individuals with Trisomy 21 (Ts21) develop craniofacial abnormalities including reduced maxillary length, altered frontomaxillary facial angles and short, broad heads (1–4). These developmental craniofacial differences preface those seen in newborn, children and adult humans with DS including midface hypoplasia, a small oral cavity, brachycephaly and a generalized reduction in facial dimensions due to decreased growth rates and increased fluctuating asymmetry of facial soft tissues associated with decreased developmental homeostasis (4–8). Ts21 results in altered craniofacial

Received: June 22, 2016. **Revised:** August 17, 2016. **Accepted:** September 1, 2016

morphogenesis and growth that may impact orofacial structure or function, potentially resulting in eating, breathing and speech impairments (9–11).

Ts65Dn mice are the most widely used model of DS, have three copies of orthologs to ~50% of the genes on human chromosome 21 (Hsa21) and exhibit phenotypes associated with DS including craniofacial dysmorphology, skeletal alterations and cognitive deficits (7,12,13). Newborn Ts65Dn mice exhibit reduced dimensions along the rostrocaudal and mediolateral axes of the face and palate, anterior and posterior neurocranium, and mandible (14). Adult Ts65Dn mice exhibit increased neurocranial widths (i.e. brachycephaly), a flattened occiput and an overall reduction in size of much of the craniofacial skeleton; including the midface, maxilla, mandible, facial height and interorbital breadth (7).

Neural crest cells (NCC) are an important component of craniofacial development and contribute to the majority of the bone, cartilage, connective tissue and peripheral nervous tissue in the craniofacial complex (15–17). Using the Ts65Dn DS mouse model, we provided the first experimental evidence that trisomy disrupts NCC that would lead to the craniofacial abnormalities associated with DS (18). We found that the trisomic mandibular precursor, or first pharyngeal arch (PA1), was smaller in size and had fewer NCC by embryonic day 9.5 (E9.5). Additional deficits were quantified in trisomic embryonic cranial NCC generation, migration and proliferation (18). In later development, Ts65Dn mice also displayed a smaller mandibular precursor than normal E13.5 embryos (19). These and other developmental changes result in modified craniofacial structures in newborn and adult Ts65Dn mice that are similar to those found in humans with DS (7,14).

It has been hypothesized that differential expression of *DYRK1A* (dual-specificity tyrosine-(Y)-phosphorylation regulated kinase 1A), a gene found in three copies in humans with Ts21 as well as in Ts65Dn mice, significantly affects many DS traits including craniofacial and neurological malformations (20). DYRK1A is a serine–threonine kinase that regulates many downstream proteins and transcription factors (20,21) and affects cell proliferation, differentiation and survival (22–24). Transgenic mice with increased dosage of *Dyrk1a* show developmental delay, motor impairment, learning and memory deficiencies as well as reduced bone mass and altered bone structure (21,25–28) similar to developmental, cognitive and morphological phenotypes observed in Ts65Dn mice. We have shown that eliminating one copy of *Dyrk1a* in otherwise trisomic Ts65Dn mice normalizes the appendicular skeleton (29). One of the many mechanisms regulated by Dyrk1a via protein phosphorylation is the nuclear localization and activity of nuclear factor of activated t-cells (Nfat) transcription factor. Dyrk1a may control bone development and homeostasis through the Nfat pathway (28). Nfat has not been widely studied *in vivo* in bone, but Nfatc2/4$^{-/-}$ mice exhibit craniofacial abnormalities (20), suggesting that the Nfat pathway, in addition to other pathways, may be involved in the morphogenesis, growth and maintenance of the craniofacial complex.

Epigallocatechin-3-gallate (EGCG) is a known inhibitor of Dyrk1a protein kinase activity. Dyrk1a is an excellent drug target because small molecules like EGCG may attach to the ATP binding site of the Dyrk1a protein kinase (30). EGCG crosses the placental and blood/brain barriers (31,32). Treatment with an EGCG-containing supplement (Mega Green Tea Extract—45% EGCG, 98% polyphenols) in adulthood transiently improved spatial learning, thigmotaxis and novel object cognitive deficits in Ts65Dn and *Dyrk1a* transgenic mice (33) and adult hippocampal neurogenesis in *Dyrk1a* transgenic mice. Treatment with a similar EGCG-containing supplement in humans with DS showed some transient improvements in episodic and working memory (33), and with additional cognitive training, improvement of some secondary cognitive measures of executive functioning and adaptive behavior in functional academic skills (34). We have used a pure EGCG treatment for 3 weeks in adolescent mice to improve appendicular bone mineral density and trabecular skeletal phenotypes in Ts65Dn DS mice (29). A perinatal pure EGCG treatment transiently improved hippocampal neurogenesis (35). Yet, the aforementioned therapies with EGCG or EGCG-containing supplements are not likely to produce a permanent change in either cellular structure of the brain or cognitive function. Conversely, EGCG treatment during development and maturation of critical cellular and organ systems has the potential to induce permanent changes in adult mice or humans.

We hypothesized that increased Dyrk1a activity during embryonic trisomic development, through interactive effects including changes in Nfat nuclear localization, significantly contributes to DS craniofacial dysmorphology in Ts65Dn mice and individuals with Ts21. By altering Dyrk1a expression, either by inhibiting activity or by lowering gene dosage during embryonic development, we hypothesized that craniofacial skeletal dysmorphology would be permanently improved in the Ts65Dn DS mouse model. Our work delineating the time and tissue specificity of the NCC deficit related to DS led us to propose that prenatal treatment with EGCG during embryonic stages, when trisomy disrupts the NCC population, would result in improved craniofacial structure in both embryonic and adult stages and may correct gene expression changes caused by trisomy. We further hypothesized that elimination of one copy of *Dyrk1a* in an otherwise trisomic animal would result in improved craniofacial anatomy in Ts65Dn mice. We report herein the effect of EGCG treatment and reduction of *Dyrk1a* copy number on the trisomic craniofacial phenotypes associated with DS.

Results

Expression of *Dyrk1a* and *Rcan1* RNA is dysregulated in the Ts65Dn E9.25 and E9.5 PA1 and neural tube

Dysregulation of *Dyrk1a* and *Regulator of Calcineurin 1 (Rcan1)* have been hypothesized to influence craniofacial phenotypes associated with DS (20), and we hypothesized that these trisomic genes may be involved in the NCC deficit of E9.5 Ts65Dn embryos (18). Before the NCC deficit is established in trisomic embryos at E9.25 (15–19 somites), trisomic embryos displayed decreased expression of *Dyrk1a* RNA (relative Ts65Dn to euploid expression) and increased *Rcan1* RNA expression in both the E9.25 PA1 and neural tube (NT) (Fig. 1A). At E9.5 (21–24 somites), when the NCC deficit is apparent, *Dyrk1a* RNA expression was upregulated and *Rcan1* RNA expression was downregulated in the E9.5 PA1 and NT (Fig. 1B).

Nfat localization not altered in E9.5 or E13.5 PA1

To determine the effects of increased copy number of *Dyrk1a* and *Rcan1* on the cellular localization of Nfatc1 protein in trisomic craniofacial precursors, we conducted immunohistochemistry on the PA1 of E9.5 and E13.5 Ts65Dn and euploid embryo sections. Ts65Dn embryos exhibited a similar amount of nuclear Nfatc1 protein in the PA1 cells when compared with euploid littermates at E9.5 (Supplementary Material, Fig. S1; $P = 0.22$). These results suggest that the increased *Dyrk1a* RNA expression and reduced

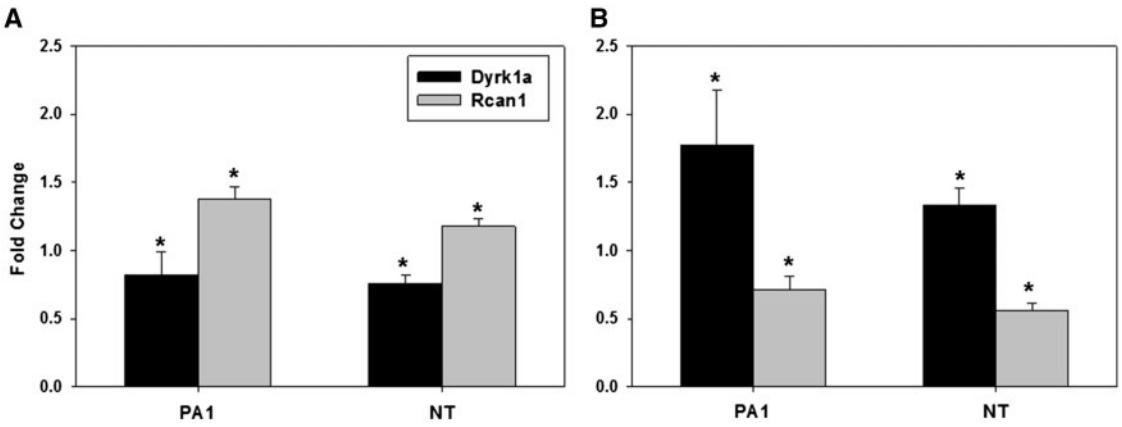

Figure 1. Dysregulation of RNA expression from Hsa21 homologous genes found in three copies in Ts65Dn mice occurs in the PA1 and NT early in development. (**A**) *Dyrk1a* RNA expression was significantly downregulated in the E9.25 PA1 and NT of trisomic embryos, whereas *Rcan1* RNA expression was significantly upregulated in both the E9.25 PA1 and NT in trisomic embryos ($N = 5$ euploid, 5 Ts65Dn PA1; 5 euploid, 5 Ts65Dn NT). (**B**) Conversely, *Dyrk1a* RNA expression was upregulated in the E9.5 PA1 and NT in trisomic embryos relative to euploid littermates, whereas *Rcan1* RNA expression was downregulated in these tissues ($N = 7$ euploid, 7 Ts65Dn PA1; 5 euploid, 5 Ts65Dn NT). For statistical analysis, two-tailed Student's *t*-tests were performed. Statistical significance is annotated as * for $P \leq 0.05$. Error bars indicate standard error of the mean.

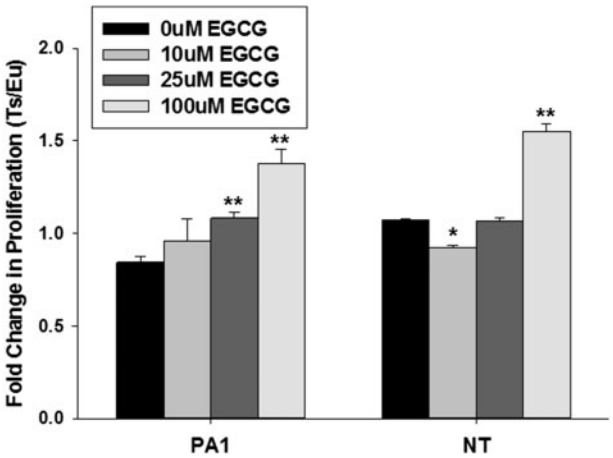

Figure 2. Ts65Dn PA1 cells displayed a proliferation deficit which can be overcome with EGCG treatment. Cells from the PA1 of E9.5 Ts65Dn embryos displayed impaired proliferation compared with euploid cells ($P \leq 0.01$) ($N = 8$ euploid, 7 Ts65Dn). A significant cellular proliferation occurred with 25 μM EGCG treatment for 4 h ($P \leq 0.001$) ($N = 10$ euploid, 10 Ts65Dn). Addition of 100 μM EGCG led to an increase in proliferation above euploid levels ($P \leq 0.001$). Cells derived from the NT displayed no deficit in proliferation, but were still affected by EGCG treatment. A dose of 10 μM ($N = 10$ euploid, 10 Ts65Dn) appeared to adversely affect proliferation of cells from NT ($P \leq 0.01$), whereas 25 μM EGCG produced no change from untreated trisomic cells ($P = 0.89$). A significant increase in cells was seen, however, in cells treated with 100 μM EGCG ($N = 10$ euploid, 10 Ts65Dn) to above euploid levels ($P \leq 0.001$). For statistical analysis, a two-tailed Student's *t*-test was performed. Statistical significance is annotated as * for $P \leq 0.05$ and ** for $P \leq 0.001$ with respect to the untreated cells by tissue type. Error bars indicate standard error of the mean.

Rcan1 RNA expression in the E9.5 PA1 of Ts65Dn as compared with euploid embryos do not affect Nfatc1 nuclear localization in the PA1 cells at this time point. Similar to what was observed in the E9.5 PA1, no significant differences in Nfatc1 nuclear localization were found between the E13.5 mandibular precursor cells of Ts65Dn and euploid embryos, when we have shown a reduced expression of *Dyrk1a* RNA and increased expression of *Rcan1* RNA in the trisomic mandibular precursor (19) (Supplementary Material, Fig. S2; $P = 0.37$). Nfatc2 is involved in cartilage development (36) and may be an alternative pathway contributing to the Ts65Dn mandibular phenotype. Nuclear localized Nfatc2 protein was also not significantly different in the E13.5 mandibular precursor cells between euploid and trisomic embryos (data not shown). Together these data suggest that trisomic Dyrk1a- and Rcan1-mediated regulation of the Nfat nuclear protein localization in cells of the mandibular precursors is likely not a factor in the altered development of the Ts65Dn mandibular phenotype at these two developmental time points.

EGCG ameliorates Ts65Dn PA1 cellular proliferation and migration deficits *in vitro*

Due to the aberrant cellular phenotype in the trisomic PA1, we looked at the biological activity of cells that comprise this structure. Cells isolated from trisomic E9.5 embryonic PA1 showed significantly less proliferation than those from euploid PA1 *in vitro* (Fig. 2). Treatment of E9.5 PA1 cells with 10 μM EGCG *in vitro* led to not only a significant increase in proliferation of trisomic cells from the PA1 but also a significant decrease in the proliferation of trisomic cells from the NT. Treatment with 25 μM EGCG was sufficient to ameliorate the trisomic E9.5 PA1 proliferation deficit without altering NT proliferation significantly. In addition, treatment with 100 μM EGCG led to significantly higher proliferation in both E9.5 PA1 and NT cells than those of euploid animals.

Ts65Dn and euploid E9.5 PA1 and NT cellular migration was assessed using the scratch assay, in conjunction with dimethyl sulfoxide (DMSO) or EGCG treatment for 4 h. Ts65Dn E9.5 PA1 cells treated with 10 μM EGCG showed a significant increase in migration (average number of cells entering the open space) over euploid levels compared with DMSO treatment over the 72 h of the assay (Fig. 3A). This concentration of EGCG treatment led to an increase in migration of Ts65Dn NT cells that nearly reached euploid levels after 72 h in culture (Fig. 3B). The ratio of trisomic to euploid migration of E9.5 PA1 and NT cells was normalized with 10 or 25 μM EGCG treatment (Fig. 3A and B).

Harmine ameliorates Ts65Dn PA1 proliferation deficits *in vitro*

Similar to EGCG, harmine binds the ATP-binding pocket of Dyrk1a and inhibits its activity (37). Harmine was also assessed

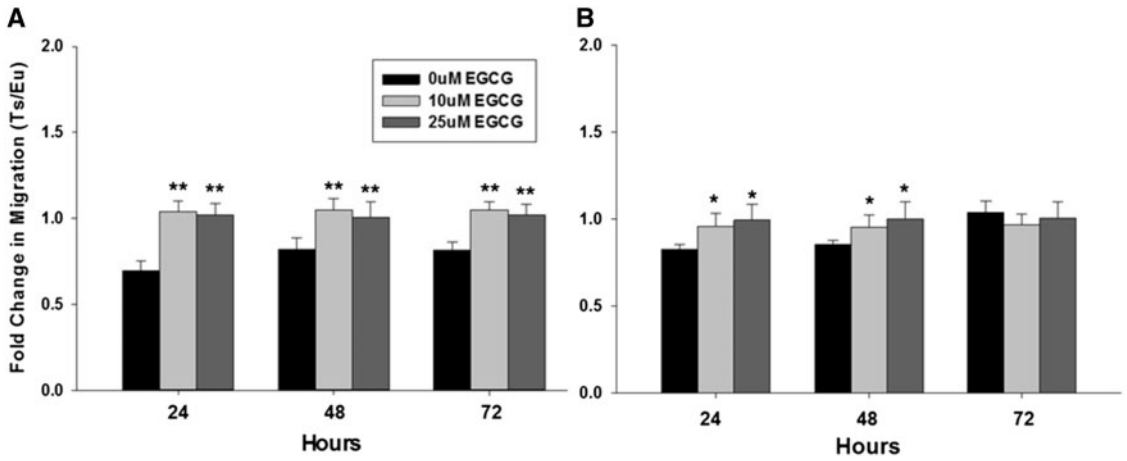

Figure 3. Ts65Dn PA1 and NT cells displayed migration deficits at E9.5 which can be overcome with EGCG treatment. (**A**) Cells from the PA1 of Ts65Dn E9.5 embryos displayed an initial cellular migration deficit (average number of cells traveling into the space made by the scratch, $P \leq 0.001$) which was not overcome through the progression of the scratch assay ($N = 11$ euploid, 8 Ts65Dn). However, treatment with both 10 μM ($P \leq 0.01$) ($N = 8$ euploid, 8 Ts65Dn) and 25 μM EGCG ($P \leq 0.01$) ($N = 7$ euploid, 7 Ts65Dn) was sufficient to rescue this cellular migration deficit within 24 h. Migration trends were maintained in the PA1 at 48 and 72 h ($P \leq 0.01$ for all conditions). (**B**) Cellular migration in the NT was deficient at 24 h postassay initiation, but appeared to reach euploid levels of migration by the completion of the assay. Treatment with 10 μM ($P \leq 0.05$) and 25 μM ($P \leq 0.05$) rescued this initial migration deficit by 24 h through the termination of the assay. For statistical analysis, two-tailed Student's *t*-tests were performed. Statistical significance is annotated as * for $P \leq 0.05$ and ** for $P \leq 0.01$ with respect to untreated cells by tissue type. Error bars indicate standard error of the mean.

for biological effects in cells from E9.5 Ts65Dn PA1 and NT. Cellular proliferation in both trisomic and euploid E9.5 PA1 and NT cells was amplified with increasing concentrations of harmine (Supplementary Material, Fig. S3).

In vivo EGCG treatment of Ts65Dn offspring normalizes some trisomic embryonic structures to euploid levels

Due to the abrogation of trisomic cellular phenotypes upon EGCG treatment *in vitro*, Ts65Dn and euploid pregnant females were treated with EGCG or phosphate buffered saline (PBS) by oral gavage to determine how EGCG affects embryos *in vivo*. Pregnant Ts65Dn or euploid mothers were given PBS or 200 mg/kg EGCG twice daily on gestational days 7 and 8 (E7 and E8). EGCG treatment did not adversely affect litter size (Supplementary Material, Fig. S4) or average somite numbers between embryo genotypes and treatments (Supplementary Material, Fig. S5), though we did observe increased variability in somite numbers from mothers receiving EGCG (Supplementary Material, Fig. S6).

In 21–24 somite E9.5 embryos from mothers receiving EGCG treatment, trisomic PA1 volume increased significantly compared with Ts65Dn embryos receiving PBS alone, but not to the size of the E9.5 euploid embryonic PA1 that received PBS. Furthermore, euploid E9.5 embryos receiving EGCG showed a significant increase in PA1 volume compared with euploid embryos receiving PBS (Fig. 4A). Trisomic E9.5 embryos receiving EGCG showed an increase in NCC number to near PBS-treated euploid levels (Fig. 4B). Euploid embryos receiving EGCG also displayed an increase in NCC number in the PA1 compared with euploid embryos receiving PBS. E9.5 trisomic embryos receiving PBS were significantly smaller than euploid embryos receiving PBS, and giving EGCG to trisomic embryos was not sufficient to change this relationship (Fig. 4C). However, E9.5 euploid embryos receiving EGCG displayed a significantly increased total embryo volume as compared with euploid embryos receiving PBS (Fig. 4C).

In vivo EGCG treatment alters gene expression in pathways implicated in trisomic craniofacial development

Relative RNA expression (to that of untreated euploid embyros) of *Dyrk1a*, *Rcan1*, *Shh* (sonic hedgehog), *Gli1* (glioma-associated oncogene family zinc finger 1), *Ptch1* (patched 1) and *Ets2* (V-ets avian erythroblastosis virus E26 oncogene homolog 2), all of which have been implicated in DS craniofacial development or developmental pathways (20,38,39), was examined in the PA1 of E9.5 embryos obtained from mothers receiving EGCG or PBS on E7 and E8. Significant decreases in *Ptch* and *Ets2* RNA expression and significant increases in *Rcan1* and *Shh* RNA expression to euploid levels were observed in the EGCG-treated trisomic PA1 relative to original trisomic baseline expression values in untreated embryos (Fig. 5).

Elongated treatment of lower dose EGCG has little effect on trisomic embryos

We hypothesized that treatment of pregnant Ts65Dn mothers with a lower dose of EGCG from the start of pregnancy to E9.5 might more comprehensively correct the cellular and volumetric deficits of developing trisomic PA1 and embryos to resemble measurements in euploid littermates. When pregnant Ts65Dn mice were given 0.124 mg/ml EGCG from E0 to E9, females ingested ~12 mg/kg/day EGCG (taking into account degradation of EGCG) (40). There was no difference in the amount of EGCG or water (control) that the pregnant females drank. There was a significant increase in PA1 volume in euploid E9.5 embryos from trisomic mothers [Eu/(Ts)] compared with untreated embryos of the same genotype ($P = 0.046$) (Fig. 6A). This elongated treatment of a lower dosage of EGCG, however, did not lead to significant improvements in the number of NCC in the PA1 (Fig. 6B) nor total embryo volume of E9.5 trisomic embryos compared with those treated with water (Fig. 6C).

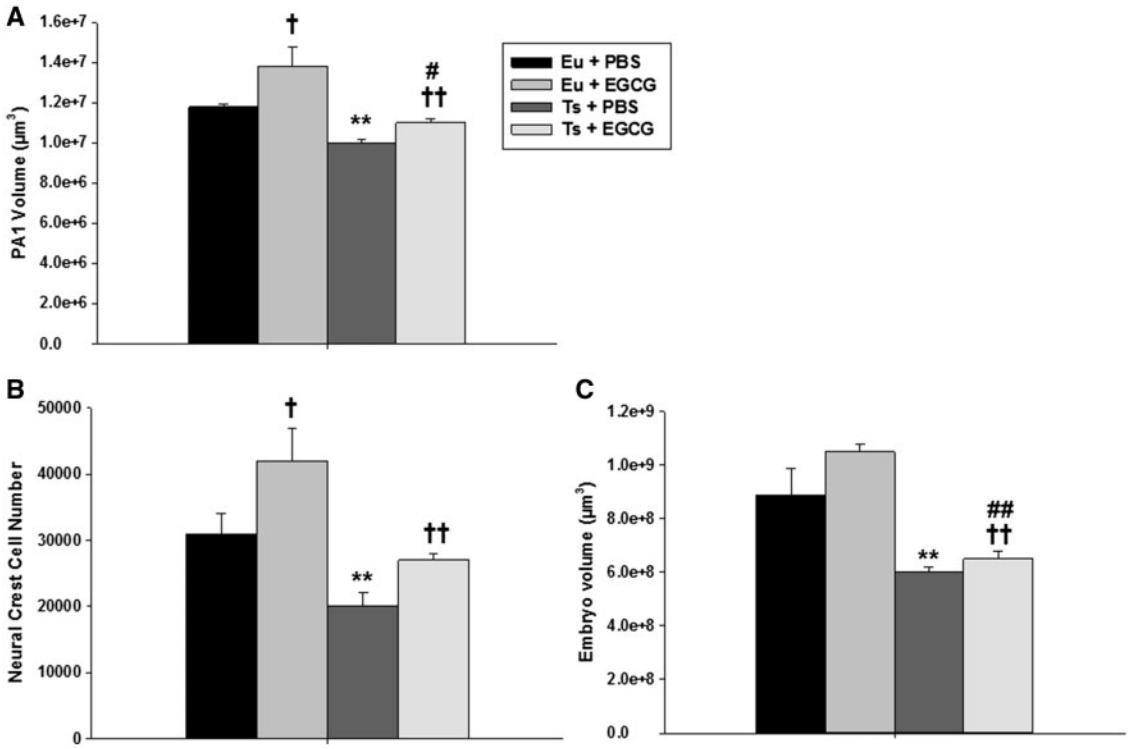

Figure 4. Effects of EGCG treatment given at E7–E8 on E9.5 PA1 volume, NCC number and embryo volume. (**A**) Ts65Dn embryos receiving PBS *in utero* displayed a smaller PA1 volume than euploid embryos receiving PBS ($P \leq 0.001$). Treatment of Ts65Dn embryos with EGCG improved PA1 volume to above baseline trisomic PA1 volume ($P \leq 0.001$), but not to PBS-treated euploid PA1 volume. Treatment of euploid embryos with EGCG led to increased PA1 over non-treated euploid PA1 volume ($P \leq 0.05$). (**B**) Treatment of trisomic embryos with EGCG ameliorated the NCC deficit to euploid levels ($P = 0.082$). Treatment of euploid embryos with EGCG, led to an increase in NCC above euploid levels ($P \leq 0.05$). (**C**). Treatment of trisomic embryos with EGCG did not lead to a significant increase in volume compared euploid embryos, but did increase embryonic volume in comparison to PBS-treated trisomic embryos. Euploid embryos treated with EGCG displayed increased embryo volume compared with euploid-treated PBS embryos, but this value was not significant ($P = 0.092$) (Ts65Dn $N = 4$, Ts65Dn + EGCG $N = 4$, euploid $N = 4$, euploid + PBS $N = 4$). For statistical analysis, two-tailed Student's *t*-tests were performed. Statistical significance is annotated as ** for $P \leq 0.001$ for untreated trisomic versus euploid, †$P \leq 0.05$ and ††$P \leq 0.001$ for EGCG-treated versus -untreated of the same genotype, and #$P \leq 0.05$ and ##$P \leq 0.001$ for trisomic EGCG-treated versus euploid-untreated comparisons. Error bars indicate standard error of the mean.

Effects of EGCG treatment or *Dyrk1a* copy number on postnatal craniofacial structure

We tested whether prenatal EGCG treatment or a reduction in *Dyrk1a* dosage would have a permanent effect on postnatal craniofacial structure in trisomic and euploid offspring at 6 weeks of age. Craniofacial structure from trisomic and euploid offspring that received EGCG treatment at E7–E8 or offspring from Ts65Dn × *Dyrk1a*$^{+/-}$ matings was examined at 6 weeks of age. Using Euclidian distance matrix analysis (EDMA) (7,41,42), a total of 231 unique linear distance measures were evaluated from each mouse skull, and separate two-sample analyses of the cranial vault, facial skeleton, cranial base and mandible were carried out. EDMA confidence interval tests ($\alpha = 0.10$) revealed morphological patterns of variation unique to each comparison of mouse samples.

When Ts65Dn and euploid offspring that received PBS from E7-E8 were compared, differences in the percentage of significant linear distances were notable in the cranial base, cranial face, mandible and cranial vault (Table 1). The great majority of significant differences across the craniofacial complex was larger in euploid as compared with Ts65Dn mice (Fig. 7A). When Ts65Dn + EGCG were compared with euploid + PBS mice, a reduced percentage of significant differences was most notable in the cranial vault as compared with the previous comparison. The great majority of significant differences was larger in the euploid compared with the Ts65Dn + EGCG mice; however, differences localized to the anterior cranial vault and zygomatic bones were smaller in the euploid relative to the Ts65Dn + EGCG mice (Fig. 7B). Very few differences were seen when Ts65Dn mice that received EGCG were compared with Ts65Dn mice that received PBS (Fig. 7C). The most significant differences were seen across all dimensions of craniofacial regions when euploid + EGCG were compared with euploid + PBS mice (Table 1). The great majority of significant differences was larger in the euploid + EGCG mice as compared with euploid + PBS mice; however, four measures localized to the anterior and posterior cranial vault including mediolateral measures of the frontal and zygomatic bones and an anterioposterior measure of the interparietal bone were significantly smaller in the euploid + EGCG relative to euploid + PBS mice (Fig. 7D).

Fewer significant differences were seen when one copy of *Dyrk1a* was removed from otherwise trisomic Ts65Dn mice (Ts65Dn,*Dyrk1a*$^{+/-}$—two copies of *Dyrk1a*) or euploid mice (euploid,*Dyrk1a*$^{+/-}$—one copy of *Dyrk1a*) (Table 1). When euploid and Ts65Dn mice from a (Ts65Dn × *Dyrk1a*$^{+/-}$) mating were compared, relatively few significant differences were found across the face, cranial base and mandible, but numerous significant difference occurred across the cranial vault (Table 1 and Fig. 7E). Unexpectedly, almost all significant differences were smaller in the euploid as compared with Ts65Dn mice. No significant differences were seen in the cranial base, and few facial, mandibular or cranial vault differences were found when comparing Ts65Dn,*Dyrk1a*$^{+/-}$ and euploid mice (Fig. 7F). In Ts65Dn,*Dyrk1a*$^{+/-}$ mice, differences in the cranial vault were

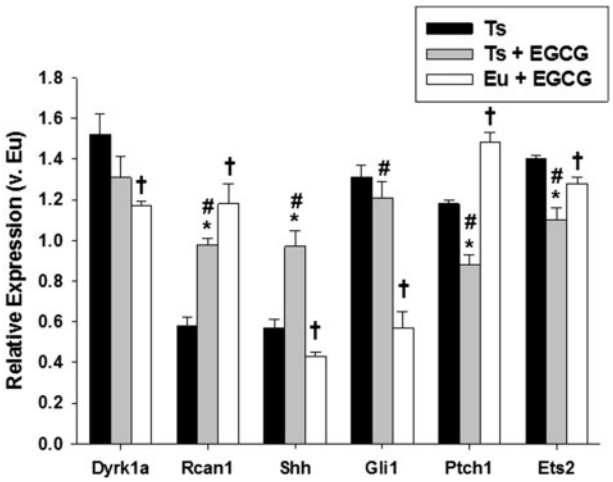

Figure 5. EGCG exposure leads to alterations of RNA expression from genes involved in pathways impacting craniofacial development E9.5 PA1. Baseline expression of RNA encoded by *Dyrk1a*, *Rcan1*, *Shh*, *Gli1*, *Ptch1* and *Ets2* quantified as cDNA by qRT-PCR revealed alterations in expression from euploid values (equivalent to a relative expression value of 1). RNA expression from these genes was altered in several cases in E9.5 trisomic PA1 receiving EGCG treatment *in utero* with most achieving near euploid values of relative expression. For statistical analysis, two-tailed Student's *t*-tests were performed. Statistical significance is annotated as * for $P \leq 0.05$ for Ts65Dn + PBS versus Ts65Dn + EGCG, †$P \leq 0.05$ for Ts65Dn + PBS untreated versus euploid + EGCG and #$P \leq 0.05$ for Ts65Dn + EGCG versus euploid + EGCG. Error bars indicate standard error of the mean.

largely corrected (Fig. 7F) as compared with results from the comparisons of Ts65Dn and euploid mice from a (Ts65Dn × *Dyrk1a*$^{+/-}$) mating (Fig. 7E, Table 1). When Ts65Dn,*Dyrk1a*$^{+/-}$ and Ts65Dn mice were compared, one fewer copy of *Dyrk1a* on an otherwise trisomic background unexpectedly caused the majority of significant linear distances to be smaller in the Ts65Dn,*Dyrk1a*$^{+/-}$ relative to the Ts65Dn mice (Fig. 7G). Very few significant differences were found when euploid (two copies *Dyrk1a*) and euploid,*Dyrk1a*$^{+/-}$ (one copy *Dyrk1a*) were compared (Fig. 7H).

Effects of EGCG treatment or *Dyrk1a* copy number on postnatal mass and airway volume

Similar to previous studies (43), Ts65Dn mice had a significantly smaller mass than euploid 6-week-old littermates when treated with PBS or when compared with littermates with *Dyrk1a* copy number variants (Table 2). Treatment with EGCG significantly reduced the mass of Ts65Dn and euploid littermates. Consistent with previous results (29,44), Ts65Dn,*Dyrk1a*$^{+/-}$ mice exhibited significantly increased mass when compared with Ts65Dn littermates, and euploid,*Dyrk1a*$^{+/-}$ mice were significantly smaller than euploid littermates. Nasopharyngeal airway volume was not significantly different between Ts65Dn and euploid mice or between Ts65Dn and Ts65Dn mice receiving EGCG. There were no significant differences in nasopharyngeal airway volume between Ts65Dn and Ts65Dn,*Dyrk1a*$^{+/-}$ littermates, but euploid,*Dyrk1a*$^{+/-}$ mice had a significantly smaller nasopharyngeal airway volume than euploid mice (Table 2).

Discussion

Expression of *Dyrk1a* RNA was decreased in the PA1 and NT of Ts65Dn as compared with euploid embryos at E9.25 but significantly increased in the same structures at E9.5. *Rcan1* RNA expression exhibited the opposite effect at these time points. We have previously shown that *Dyrk1a* RNA expression was significantly decreased and *Rcan1* expression increased in the E10 PA1 of Ts65Dn relative to euploid embryos (45) and both *Dyrk1a* and *Rcan1* exhibited significantly increased RNA expression in the Ts65Dn as compared with euploid E13.5 mandibular precursor (19). Taken together, these data indicate that expression of trisomic *Dyrk1a* and *Rcan1* RNA are not consistently increased or decreased in the mandibular precursor of developing Ts65Dn embryos. These data may help clarify why reducing *Dyrk1a* copy number in Ts65Dn mice throughout development does not seem to significantly normalize the entire mandibular structure in 6-week-old Ts65Dn mice. Changes in RNA expression of *Dyrk1a* and *Rcan1* in trisomic embryos appear to be temporally specific in the developing mandible. Furthermore, the dysregulation of *Dyrk1a* and *Rcan1*, both hypothesized to be linked to altered *Nfatc* expression in trisomic animals (20), do not seem to affect Nfatc nuclear localization in mandibular precursor cells at either E9.5 or E13.5. It may be that Nfatc cellular localization or expression is dysregulated at other time points during mandibular development or not altered by trisomic genes. We have previously shown that Nfatc nuclear localization is not altered in trisomic bone development at the time of the cartilage anlagen (E13.5) (46).

This study shows that a temporally specific prenatal EGCG treatment improves some craniofacial dysmorphology associated with DS in Ts65Dn embryos and mice. EGCG and harmine, both inhibitors of Dyrk1a activity (47), effectively improve NCC-related deficits in proliferation and migration *in vitro* in PA1 cells from Ts65Dn E9.5 embryos. *In vivo* treatment with EGCG at E7 and E8, around the time of the developing NCC deficit, appears to improve some of the NCC embryonic dysmorphology, especially in PA1 volume and NCC number in Ts65Dn E9.5 embryos. Gene expression was also altered by EGCG treatment and essentially normalized *Rcan1*, *Shh*, *Ptch1* and *Ets2* RNA expression—all of which are genes hypothesized to be related to some DS craniofacial deficits (18,38,39,48). EGCG treatment and Dyrk1a activity have been shown to be connected to and modulate the Shh pathway (49–51). However, a longer lasting EGCG treatment at a lower dose (E0–E9) did not have the same corrective effect on the trisomic embryonic structure at E9.5. These results suggest that timing and dosage of EGCG treatment are important in treating DS-related phenotypes.

The embryonic changes caused by prenatal EGCG treatment at E7–E8 appear to improve some craniofacial structures, particularly the cranial vault, in adult trisomic mice. The morphometric analysis used in this study (i.e. EDMA) assessed local form differences by comparing all unique linear measures across the cranial vault, face, base and mandible. Because of the potential for a large number of linear measures to significantly differ, it is useful to consider patterns of significant differences across craniofacial structures and to calculate summary statistics based on significant results. Here, we counted the number of significant linear distances in a particular region and divided this value by the total number of unique linear distances for that particular region (i.e. the number of linear distances that could have potentially been significantly different) to determine the percentage of significant differences for each craniofacial region (Table 1). This summary statistic is useful for comparing global results on a region by region basis from multiple two-sample EDMA analyses (4,52), although specific dimensions of interest for each region should be explored using local results (Fig. 7). EGCG treatment of Ts65Dn embryos reduced the percentage of significant differences from 19% to 14% in the cranial base, from 32% to 26% in

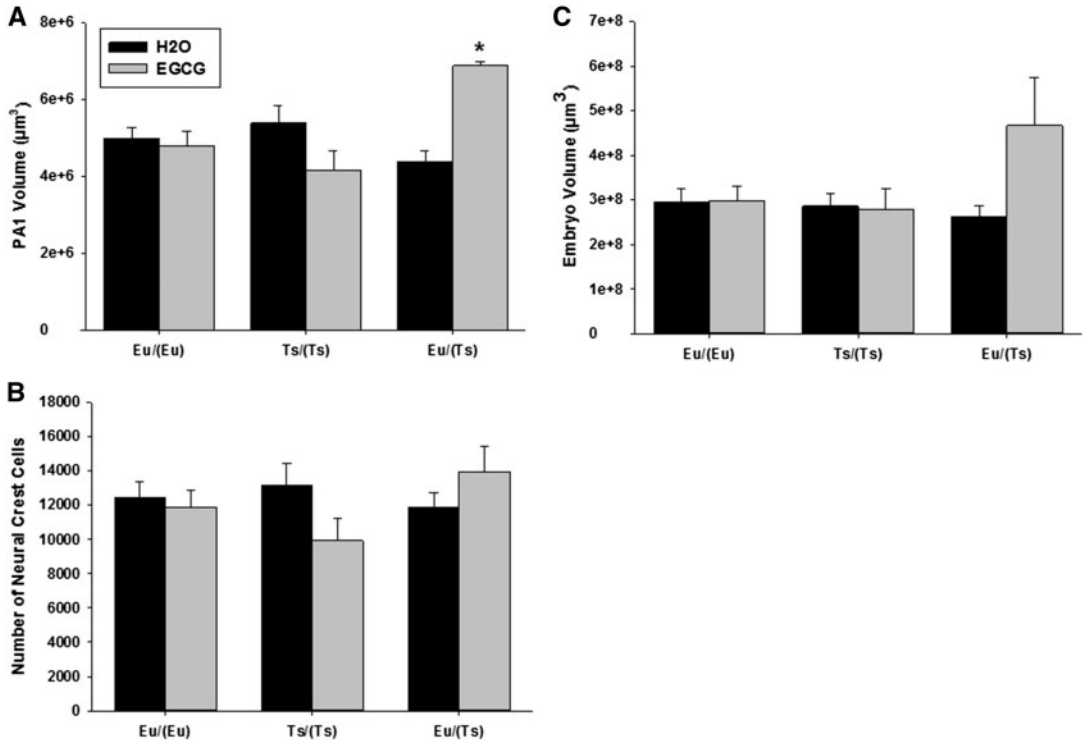

Figure 6. Effects of EGCG treatment given at E0–E9.5 on E9.5 PA1 volume, NCC number and embryo volume. Ts/(Ts), trisomic embryos from Ts65Dn mothers; Eu/(Ts), euploid embryos from Ts65Dn mothers; Eu/(Eu), euploid embryos from euploid B6C3F1 mothers. Ts/(Ts) + H20: $n = 9$; Ts/(Ts) + EGCG: N = 5; Eu/(Ts) + H20: N = 6; Eu/(Ts) + EGCG: N = 9; Eu/(Eu) + H20: N = 8; Eu/(Eu) + EGCG: N = 7. (**A**) No significant differences were seen in the PA1 volume of EGCG-treated trisomic Ts/(Ts) or euploid Eu/(Eu) embryos compared with untreated embryos ($P = 0.058$). PA1 volume was significantly increased in EGCG-treated euploid embryos [Eu/(Ts)] compared with untreated embryos [Eu/(Ts)]. (**B**) EGCG treatment from E0 to E9.5 at ~12 mg/kg/day did not significantly alter the number of NCC in any treatment groups compared with untreated embryos. The slight but non-significant decrease in NCC in EGCG-treated Ts/(Ts) embryos was likely due to a lower average somite number in this group compared with water treated embryos ($P = 0.0613$). (**C**) No differences were found between treated and untreated embryo volume of any trisomic or euploid embryos. Statistical significance is annotated as * for $P \leq 0.05$. Error bars indicate standard error of the mean.

the face and from 22% to 5% in the cranial vault in adult mice. This suggests that EGCG treatment slightly normalized cranial base and face morphology and considerably improved cranial vault morphology. In contrast to the results from our embryonic study, EGCG treatment did not significantly improve the overall mandibular dysmorphology in 6-week trisomic animals. It may be that prenatal treatment with EGCG has a larger effect on trisomic NCC precursors that are components of other parts of the craniofacial skeleton and therefore developmentally integrated, whereas the mandible is developmentally modular and therefore less affected by treatments influencing development of other craniofacial structures such as the cranial vault, face and base. Overall the results imply that EGCG treatment at E7–E8 improves some craniofacial morphology in Ts65Dn mice, especially for the cranial vault, but does not entirely correct craniofacial structural abnormalities attributed to trisomy.

Normalization of *Dyrk1a* to two copies in otherwise trisomic Ts65Dn mice did not fully correct craniofacial dysmorphology associated with DS. Yet, our data indicate that trisomic *Dyrk1a* may be important for morphogenetic events that give rise to the shape and size of the cranial vault. Comparisons of euploid mice with Ts65Dn (three copies *Dyrk1a*) and Ts65Dn,*Dyrk1a*$^{+/-}$ (two copies *Dyrk1a*) (Table 1 and Fig. 7E and F) unexpectedly revealed numerous smaller dimensions in euploid cranial vaults relative to Ts65Dn mice, but removal of one copy of *Dyrk1a* in Ts65Dn mice improved cranial vault morphology as evidenced by the reduction in significant cranial vault differences shown in Figure 7F relative to Figure 7E. The comparison of Ts65Dn,*Dyrk1a*$^{+/-}$ and Ts65Dn mice (Fig. 7G) yielded numerous significant cranial vault differences, but significant differences were smaller in Ts65Dn mice with only two copies of *Dyrk1a*. Furthermore, EGCG treatment at E7 and E8 corrected a large number of significant differences in the cranial vault of 6-week-old Ts65Dn mice as compared with euploid littermates given PBS (Table 1 and Fig. 7A and B). In agreement with these results, we previously found that trisomic *Dyrk1a* has a major influence on the appendicular skeleton, and that reduction of *Dyrk1a* copy number in Ts65Dn,*Dyrk1a*$^{+/-}$ mice did not restore bone mineral density in the skull and mandible to euploid levels (29). Additionally, both of the airways of Ts65Dn and euploid mice from (Ts65Dn × *Dyrk1a*$^{+/-}$) matings not carrying the null *Dyrk1a* allele were larger in magnitude in comparison with those mice with EGCG/PBS treatment. Taken together, these results underscore the complexity of the gene–phenotype analyses, and suggest that changes in trisomic *Dyrk1a* expression, either via EGCG treatment or copy number reduction, play an important role in morphogenesis and growth of the cranial vault, and perhaps to a lesser degree, other craniofacial structures. It seems likely that major primary changes in cranial vault morphogenesis and growth could produce minor changes in the face, cranial base and mandible through complex regulatory and pleiotropic interactions and integrated functional craniofacial requirements related to organ protection and mastication, but additional investigations are necessary to verify this hypothesis. A limitation of our study is that we have not shown how EGCG treatment affects Dyrk1a activity in craniofacial precursors or adult structures.

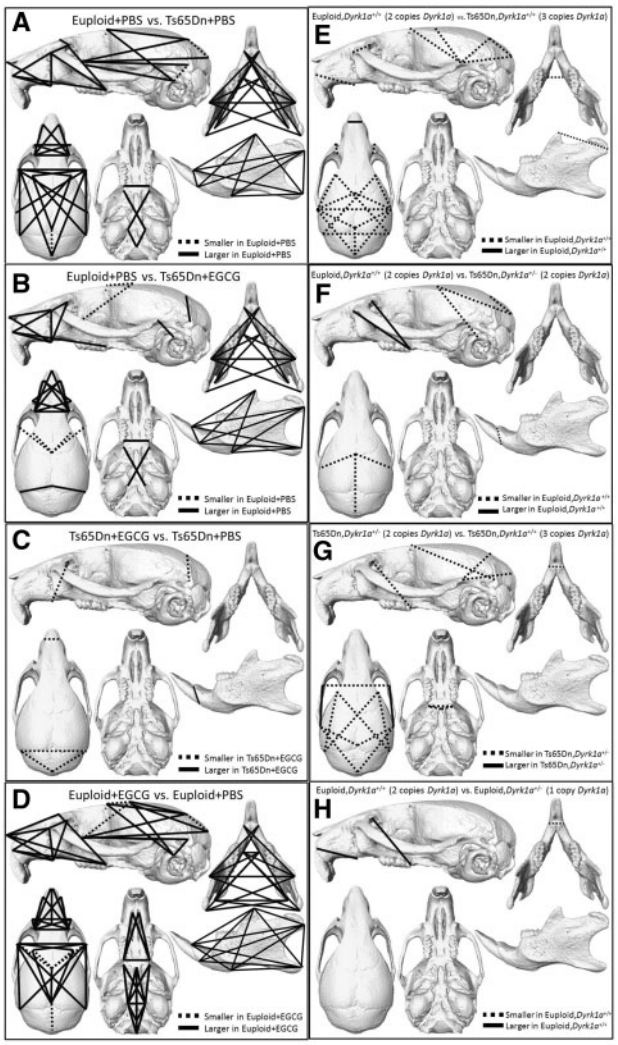

Figure 7. Craniofacial measurements of 6-week-old Ts65Dn and euploid mice with or without EGCG treatment or *Dyrk1a* genetic reduction. Linear distances that significantly differ by confidence interval testing ($\alpha = 0.10$) from two-sample EDMA comparisons of mouse cohorts are shown on lateral, superior and inferior views of the mouse cranium and superior and lateral views of the mandible. Linear distances that were significantly smaller or larger are depicted for each comparison as dashed or solid lines. (**A**) Euploid + PBS compared with Ts65Dn + PBS: significant cranial base differences were found that include anterioposterior dimensions of the palatine, basisphenoid and occipital bones. Numerous rostrocaudal, mediolateral and superioinferior differences were found across the face that include the nasal, premaxillae and maxillae bones. Many height, width and length measurements of the mandible significantly differed. Several anterioposterior, mediolateral and superioinferior measures of the cranial vault were also significant. (**B**) Euploid + PBS compared with Ts65Dn + EGCG: significant cranial base differences were found that include anterioposterior dimensions of the basisphenoid and occipital bones. Numerous length, width and height significant differences were found across the face that include the nasal, premaxillae and maxillae bones. Many anterioposterior, mediolateral and superioinferior measurements of the mandible significantly differed. Mediolateral differences in skull width were localized to the anterior portion of the cranial vault including the zygomatic arches and frontal bone and to the posterior cranial vault including the parietal bones. (**C**) Ts65Dn + EGCG compared with Ts65Dn + PBS: significant superioinferior and mediolateral facial differences including the premaxillae and nasal bones and significant cranial vault width differences localized to the interparietal bone were smaller, whereas a mandibular measure of incisor height was larger in Ts65Dn + EGCG relative to Ts65Dn + PBS mice. (**D**) Euploid + EGCG compared with euploid + PBS: differences were found across the craniofacial skeleton and localized to the nasal, premaxillae, maxillae, frontal, parietal, interparietal, occipital, basisphenoid and mandibular bones. (**E**) Euploid compared with Ts65Dn: significant differences were present along the rostrocaudal and mediolateral axes of the face including the malar process and the nasal, premaxillae and maxillae bones. Numerous significant differences were present across the cranial vault along the mediolateral and anterioposterior axes including the frontal, parietal and interparietal bones. There were significant anterioposterior differences in condylar process and coronoid process depth and significant mediolateral differences in mandibular width. (**F**) Euploid compared with Ts65Dn,*Dyrk1a*$^{+/-}$: significant facial aspects along the superioinferior–rostrocaudal dimensions including the maxillae bones were larger in euploid mice, whereas significant cranial vault dimensions along the anterioposterior and mediolateral axes including the parietal and interparietal bones and a significant mandibular measure of incisor height were smaller in euploid relative to Ts65Dn,*Dykr1a*$^{+/-}$ mice. (**G**) Ts65Dn,*Dyrk1a*$^{+/-}$ compared with Ts65Dn: significant mediolateral differences in palatine bone width were found. One superioinferior–rostrocaudal facial measure of the maxillary bone significantly differed between samples. A measure of incisor width was significant. There were numerous significant differences in mediolateral and anterioposterior cranial vault dimensions crossing the zygomatic, frontal, parietal, interparietal and squamosal bones. (**H**) Euploid compared with euploid,*Dyrk1a*$^{+/-}$: significant facial dimensions along the superioinferior and rostrocaudal dimensions including the premaxillae and maxillae bones were larger, whereas a mandibular measure of incisor width was smaller in euploid relative to euploid,*Dyrk1a*$^{+/-}$ mice.

Differences in craniofacial and airway measurements between trisomic and euploid mice from the pharmacological and genetic alterations were not expected. Ts65Dn and euploid mice from either control (PBS) treatment or that did not carry the *Dyrk1a* null allele exhibited similar overall weights at 6 weeks of age (Table 2). Yet, the craniofacial measurements in trisomic offspring (without a null *Dyrk1a* gene) from (Ts65Dn × *Dyrk1a*$^{+/-}$) matings were generally larger than euploid littermates (Fig. 7E and F). To generate the *Dyrk1a*$^{+/-}$ mice used in the breeding scheme of this study, C57BL/6-129/Ola-mixed genetic background *Dyrk1a*$^{+/-}$ mice carrying the null *Dyrk1a* allele (44,53) were bred onto a B6C3 advanced intercross background for seven or more generations. This advanced intercross background was intended to be similar to the approximate 50% B6 and 50% C3H genetic background of Ts65Dn mice. It may be that residual background 129 alleles on the normal mouse chromosome 16 (not carrying the null *Dyrk1a* allele) cause the disparate craniofacial and airway volume phenotypes observed in the trisomic and euploid offspring from the (Ts65Dn × *Dyrk1a*$^{+/-}$) matings. A possible explanation for the larger Ts65Dn cranial vault in the Ts65Dn versus euploid and Ts65Dn versus Ts65Dn,*Dyrk1a*$^{+/-}$ comparisons is that a residual background 129 allele on chromosome 16 is interacting with B6 or C3H alleles possibly indicating the interactive effects of heterotrisomy (54). Alternatively, an unknown epigenetic influence from the *Dyrk1a*$^{+/-}$ fathers may also have caused the differences in airway volume and craniofacial abnormalities seen between Ts65Dn and euploid mice from the (Ts65Dn × *Dyrk1a*$^{+/-}$) matings and mice treated with PBS. These hypotheses should be tested in offspring from additional matings of (Ts65Dn × *Dyrk1a*$^{+/-}$) mice with a similar genetic background.

Supplements containing EGCG have been shown to improve some cognitive and skeletal DS phenotypes in adult mice (33, 46). As the development of the face and brain is highly related (55–57), embryonic EGCG treatment may also alter brain morphology, which influences overall cranial vault shape during morphogenesis and growth (57). The reduction in neurocranial shape in Ts65Dn mice has been shown to correlate with the characteristic flattened occiput found in humans with DS. This region of the neurocranium overlies the cerebellum, which has reduced volume in both Ts65Dn mice and individuals with DS

Table 1. Percentage of significant differences in cranial structures of 6-week-old Ts65Dn and euploid mice with or without EGCG treatment or *Dyrk1a* dosage reduction

Comparison	Percentage of significant differences (Significantly different distances/total distances measured)			
	Cranial base	Cranial face	Mandible	Cranial vault
Ts65Dn + PBS versus euploid + PBS	19 (4/21)	32 (21/66)	52 (34/66)	22 (17/78)
Ts65Dn + EGCG versus euploid + PBS	14 (3/21)	26 (17/66)	53 (35/66)	5 (4/78)
Ts65Dn + EGCG versus Ts65Dn + PBS	0 (0/21)	5 (3/66)	3 (2/66)	3 (2/78)
Euploid + EGCG versus euploid + PBS	67 (14/21)	80 (53/66)	79 (52/66)	32 (25/78)
Ts65Dn versus euploid	0 (0/21)	8 (5/66)	3 (2/66)	17 (13/78)
Ts65Dn,*Dyrk1a*$^{+/-}$ versus euploid	0 (0/21)	5 (3/66)	3 (2/66)	5 (4/78)
Ts65Dn,*Dyrk1a*$^{+/-}$ versus Ts65Dn	10 (2/21)	3 (2/66)	5 (3/66)	12 (9/78)
Euploid,*Dyrk1a*$^{+/-}$ versus euploid	0 (0/21)	6 (4/66)	2 (1/66)	0 (0/78)

Table 2. Body weights and nasopharyngeal airway volumes of 6-week-old Ts65Dn and euploid mice with or without EGCG treatment or *Dyrk1a* dosage reduction

Genotype/treatment	Mean 6-week weight in grams (SEM) [N]	Mean airway volume in mm^3 (SEM) [N]
Ts65Dn + PBS	20.4 (0.85)[a,b] [6]	8.7 (1.76) [5]
Ts65Dn + EGCG	18.1 (0.73) [5]	7.8 (0.93) [7]
Euploid + PBS	23.3 (1.08)[c] [5]	7.3 (1.31) [5]
Euploid + EGCG	20.5 (0.57) [7]	8.7 (1.99) [7]
Ts65Dn	19.7 (0.83)[d,e] [7]	11.4 (0.78)[f] [8]
Ts65Dn,*Dyrk1a*$^{+/-}$	21.3 (0.45) [12]	9.2 (0.94) [12]
Euploid	24.7 (0.37)[g] [14]	13.0 (1.04)[h] [13]
Euploid, *Dyrk1a*$^{+/-}$	20.2 (1.57) [3]	8.9 (2.53) [7]

Data reported as mean ± (SEM).

[a] $P < 0.05$ when compared with euploid + PBS.

[b] $P < 0.001$ when compared with Ts65Dn + EGCG.

[c] $P < 0.05$ when compared with euploid + EGCG.

[d] $P < 0.05$ when compared with euploid.

[e] $P < 0.05$ when compared with Ts65Dn,*Dyrk1a*$^{+/-}$.

[f] $P = 0.06$ when compared with Ts65Dn,*Dyrk1a*$^{+/-}$.

[g] $P < 0.001$ when compared with euploid,*Dyrk1a*$^{+/-}$.

[h] $P < 0.05$ when compared with euploid,*Dyrk1a*$^{+/-}$.

(7). Future studies will need to test the hypothesis that mice with normalized cranial vault and other cranial structures may also demonstrate a correlation in improved cognitive function.

Previous research has shown that relative to euploid mice, Ts65Dn mice exhibit numerous differences across the craniofacial complex including increased cranial vault width (i.e. brachycephaly) and a generalized reduction in linear dimensions across much of the skull including the face, mandible and dimensions of the cranial vault length (7). Previous investigations of adult Ts65Dn mice aged 4–7 months found brachycephaly in the anterior and middle portions (near bregma) of the cranial vault (frontal and parietal bones) (7), but the current investigation of 6-week-old Ts65Dn mice only found increased width for some measures of the anterior vault (frontal and zygomatic bones). Brachycephaly was not reported in P0 Ts65Dn mice (14); thus, it seems likely that brachycephaly is only beginning to develop in 6-week-old mice and becomes fully developed in older Ts65Dn adult mice.

Euploid mice prenatally treated with EGCG exhibited numerous craniofacial differences affecting practically all craniofacial bones relative to euploid mice receiving PBS. The great majority of significant differences was larger in the euploid + EGCG mice, suggesting that EGCG treatment increased overall skull size relative to untreated euploid mice. This result also underscores the important, but complicated role *Dyrk1a* plays in early osteomorphogenetic developmental events and subsequent craniofacial growth. We have shown that the uterine environment of the trisomic mother does not influence gross differences in non-trisomic offspring (58) and therefore these results may have implications in treating non-trisomic offspring with EGCG.

It is possible that trisomic *Dyrk1a* expression only alters craniofacial and other precursors to specific DS-related phenotypes in a temporally and spatially specific manner. Our data suggest that an acute treatment of EGCG around the time of the NCC deficit in the trisomic PA1 affects embryonic craniofacial

precursors and structure of the adult cranial vault. Reducing trisomic *Dyrk1a* copy number did not correct embryonic Ts65Dn appendicular skeletal development (46), but did significantly correct adult skeletal phenotypes in the femur (29). In a similar manner, upregulating the Shh pathway throughout development did not correct Ts65Dn craniofacial differences but did have some effect on cognitive phenotypes (59,60). Reduction of the trisomic gene *Ets2* to normal copy number in an otherwise trisomic mouse also had minimal effect on correcting DS-related craniofacial abnormalities (38). Temporally specific regulation of *Dyrk1a* or other genetic pathways may be important to correct craniofacial and other DS-related phenotypes.

Because Ts21 can be detected prenatally, it is possible that prenatal treatments could lead to corrections of DS phenotypes (61,62). Many DS craniofacial and neurological processes are initiated or completed before birth, and a window for prenatal treatment and permanent correction of DS-related phenotypes may exist. A number of studies have examined prenatal treatments of DS phenotypes and have mostly concentrated on cognitive impairments [reviewed in (62)]. The use of prenatal supplements to correct DS phenotypes needs to be further studied in animal models, including investigations of treatment timing and dosage, and precise quantification of phenotypes before clinical trials in humans are proposed.

Materials and Methods

Generation and genotyping of mice and embryos

Female B6EiC3 Sn a/A-TS(17^{16})65Dn (Ts65Dn), B6CBA-Tg(Wnt1-lacZ)206Amc/J (Wnt1-LacZ) and male B6C3F1 mice were obtained from The Jackson Laboratory (Bar Harbor, ME). C57BL/6-129/Ola *Dyrk1a* heterozygous mutant mice (*Dyrk1a*$^{+/-}$) were obtained from Dr Mariona Arbones (Institut de Recerca Oncologica, Barcelona, Spain) (44,53). C57BL/6-129/Ola *Dyrk1a*$^{+/-}$ mice were backcrossed to B6C3F1 mice for $\geq$7 generations to parallel the genetic background of Ts65Dn mice. All mice were bred at Indiana University–Purdue University Indianapolis (IUPUI) to produce the offspring needed for this study. Female Ts65Dn mice were bred with Wnt1-LacZ or B6C3F1 males for embryonic studies. Females were checked for vaginal plugs the morning after mating to ascertain copulation. Noon on the day of the plug was established as embryonic day 0.5 (E0.5) for developing embryos. Embryos were dissected from pregnant females and were assessed for developmental stage by somite number. For E9.5 embryos (21–24 somites), pregnant mothers were euthanized between 10 am and 12 pm 9 days after the plug was visualized. For E9.25 embryos (15–18 somites), embryos were dissected at 6 am 9 days after the plug was observed. For E13.5 embryos, embryos were dissected at noon 13 days after the plug was observed. Dissected E9.25, E9.5 and E13.5 embryos were then fixed for histological analysis or PA1 and NT tissues were isolated for further investigation. Mice and embryos utilized for this study were genotyped by PCR (44,63) or fluorescence *in situ* hybridization (FISH) (64) as described. All animal use and protocols were approved by the IUPUI School of Science Institutional Animal Care and Use Committee (IACUC).

RNA isolation

The PA1 and NT of E9.5 or E9.25 embryos were dissected from the embryos in an RNase free environment using 30 gauge needles. Structures dissected were specified by a cut matching the line of the body for the PA1 and above the otic vesicle but below the midbrain for the NT. RNA was extracted using the PureLink RNA Micro Kit (Invitrogen, Carlsbad, CA) according to the manufacturer, and RNA concentration was assessed using the Nanodrop ND-1000 (Thermo Scientific, Waltham, MA).

Immunohistochemistry for Nfat expression

E9.5 and E13.5 embryos for immunohistochemistry were fixed in 4% paraformaldehyde, 5% sucrose in 0.1 M phosphate buffer pH 7.4 for 4 h and infiltrated overnight with 20% sucrose in phosphate buffer for cryo-embedding. Sections of E9.5 and E13.5 Ts65Dn and euploid embryos were permeabilized in 1× PBS with 0.5% triton X-100, washed in 1× PBS with 5% SDS for antigen retrieval, blocked with 10% donkey serum in PBS with 0.2% Triton X-100 for 1 h, and treated with rabbit polyclonal Nfatc1 (sc-13033, dilution 1:20, SCBT) or goat polyclonal Nfatc2 (CSC-1151, dilution 1:20, SCBT) diluted in blocking buffer overnight in a humidified chamber at 4 °C. Sections were washed and incubated with secondary antibody [Alexaflour 594 donkey anti-rabbit IgG (Invitrogen A21207), 1:750 and Alexafluor 488 donkey anti-goat IgG (Invitrogen A-11055), 1:750] for 1 h at room temperature and treated with Prolong gold DAPI antifade (Invitrogen, P36935), coverslipped and sealed with nail polish. Sections were examined for the nuclear localization of Nfatc1 (Nfatc1^{nuc}) in the PA1 (E9.5) or Nfatc1 and Nfatc2 in Meckel's cartilage (E13.5) using an Olympus FV-111-MPE confocal multiphoton microscope (Olympus, Center Valley, PA). Colocalization of Nfatc1/2 and DAPI in the nuclei was analyzed using Image J software (National Institute of Health, Bethesda, MD) utilizing quantitative co-localization methodology (46,65).

Cell culture of trisomic and euploid embryonic cells

For cell proliferation and migration, the E9.5 PA1 and NT were removed as described above and placed into 0.025% trypsin/0.1% collagenase/Dulbecco's phosphate-buffered saline (DPBS) for 4 min at 37 °C. Cells were triturated ~10 times per sample after incubation and then spun down at 9,280 g for 6 min. The supernatant was extracted from each tube and cells were resuspended in 50 µl of MCDM (66). Resuspended cells were plated on fibronectin-coated 96-well plates (Becton, Dickinson and Company, Franklin Lakes, NJ) (proliferation assays) or fibronectin-coated coverslips (migration assays). Cells were incubated at 5% CO_2 and 37 °C in MCDM until confluence (~12–24 h, depending on genotype and tissue). During migration assays, media changes occurred daily until assays were completed.

Proliferation assay for trisomic and euploid craniofacial precursors

Cells derived from E9.5 PA1 and NT tissues were treated with trypsin/collagenase/DPBS and grown on the 48-well plate for 24 h, then were quantified for cell titer using a hemacytometer. For proliferation assays, cells were grown to confluency on 96-well plates, transferred to 48-well plates, quantified, and replated on new wells at a density of $\sim 1 \times 10^4$. From each sample consisting of suspended cells and 200 µl MCDM, 10 µl was removed for quantification. For each cell titer, three counts were taken on a hemocytometer and averaged to obtain a cell titer per 4×10^{-3} mm^2.

Cells were allowed to grow on the plate for 8 h and then were treated with DMSO (Fair Lawn, NJ), Epigallocatechin-3-gallate

(EGCG) (Sigma, St. Louis, MO) in DMSO or harmine (Sigma), an additional inhibitor of Dyrk1a activity, in DMSO for 4 h. EGCG treatments included doses of 10, 25 and 100 μM in DMSO and harmine treatments included doses of 1 and 10 μM in DMSO. The media was replaced and cells were incubated with MCDM for 4 h. Cell Titer 96 AQueous One Solution Reagent (Promega, Madison, WI) was added to each well and one control well with media and incubated for 4 h. Proliferation was assessed using a spectrophotometer at 490 nm and plotted on a standard curve to determine the number of cells in each well. Proliferation of trisomic and euploid tissues was compared within the cell assay to determine fold changes of proliferation for each trisomic sample relative to euploid samples.

Migration assay of trisomic and euploid embryonic cells

Cells were placed on fibronectin-coated coverslips and incubated at 5% CO_2 and 37 °C for 24 h in MCDM or until confluent, and then the scratch assay was performed as described (67) by creating a diagonal scratch across the cell layer on the coverslip. Media was changed to remove debris from the scratch, and cells were treated for 4 h with DMSO, EGCG in DMSO or harmine in DMSO at concentrations described above. Migration was quantified 0, 24, 48 and 72 h after the scratch was made. MCDM was changed daily with care taken to avoid disturbing the cells. Using Image J, the number of cells in the scratch was quantified and recorded as follows: each scratch was outlined to ensure conformity among scratch width before proceeding to quantification. Any images with inconsistent scratch widths were not utilized in this analysis. Using the counting tool, the number of cells within each scratch not touching the borders outlining the scratch was quantified for three images per culture. An average of these three numbers was then used as a migration count for that sample. Migration rates were established as the number of cells fully migrated into the scratch divided by the length of time since the scratch test was initiated in hours. Trisomic migration rates were then compared with euploid migration rates of the same tissue and culture group.

Quantitative PCR to assess differential RNA expression in E9.5 PA1

RNA was converted to cDNA using the TaqMan Reverse Transcription Reagents (Applied Biosystems, Carlsbad, CA). Using this cDNA, master mixes were created for the reference gene (*actin*, *Ev1*) and target genes using TaqMan Gene Expression Master Mix (Applied Biosystems). Samples were analyzed in duplicate using the AB 7300 Real Time PCR System (Applied Biosystems). Crossing point (Cp) values from each duplicate trisomic sample were then averaged and divided by the average Cp value of the two euploid samples as performed by the 7300 System Software (Applied Biosystems). To determine a fold change, Cp values were subjected to the $2^{-\Delta\Delta Cp}$ formula as described (68). Relative quantification was performed on Ts65Dn and euploid littermate PA1 from both treated and untreated embryos. Expression was quantified for *Ev1* (*actin*, housekeeping gene), *Dyrk1a, Rcan1, Shh, Gli1, Ptch1* and *Ets2* probes (Applied Biosystems).

In vivo assessment of EGCG treatment during embryonic stages

For mice treated on embryonic (gestational) days 7 and 8 (E7 and E8), plugged female mice (Ts65Dn × Wnt1LacZ matings) were given 200 mg/kg EGCG dissolved in PBS or PBS alone twice daily at least 6 h apart by oral gavage using a 22 gauge feeding needle (69). 200 mg/kg EGCG oral gavage using a 15 mg/ml solution in a 30 g mouse results in the delivery of ∼13 μmol EGCG. Mice were given water *ad libitum* before and after the oral gavage. For mice treated from E0 to E9 (Ts65Dn or euploid × B6C3F1 matings), pregnant females were given water or 0.124 g/ml EGCG in 25 ml water in feeding tubes after the plug was detected at E0.5, without other liquid, and allowed to drink *ad libitum*. EGCG or water volume was measured and changed every 48 h. Mice were strictly monitored for general health, assessed by daily weight changes, locomotor activity in the cage, and response to handling over the 2-day period of treatment before euthanizing. On day 9 after the plug was found, females were euthanized and E9.5 embryos dissected. Embryos were processed, fixed and sectioned as previously described (18).

Stereological analysis of craniofacial precursors

Unbiased stereology (70) was used to quantify embryo and PA1 size and cell number. Systematic random sampling was used to quantify the number of cells in the PA1 and Calvalieri-point counting was utilized from volumetric measurements. Embryonic volume was assessed on every fourth section and PA1 volume and cell number were assessed sampling every third section containing PA1. Embryo volume was assessed with a frame area of 25 μm^2, 10 μm frame height, 2 μm guard height, 200 μm from spacing, 8000 μm^2 area per point and sampling from the top of the section. PA1 quantification was performed using dissectors spaced at intervals of 60 μm with dimensions of 150 μm^2 area and 8 μm depth with a 2 μm guard height. Average coefficient of error for all volumes and cell counts was $\leq$0.10. Statistical differences were determined using a one-tailed Student's *t*-test.

Assessment of embryonic EGCG treatment or *Dyrk1a* reduction on adult mice

Pregnant Ts65Dn mice were given 200 mg/kg EGCG twice daily by gavage on E7 and E8 as described above. Mice were housed until parturition, genotyped and offspring weaned after 21 days. Four types of mice were analyzed: Ts65Dn ($n=6$), Ts65Dn + EGCG ($n=7$), euploid ($n=5$) and euploid + EGCG ($n=7$). Ts65Dn mice were bred to *Dyrk1a* heterozygous knockout mice (44). Offspring from the (Ts65Dn × $Dyrk1a^{+/-}$) cross were genotyped for trisomy as well as the *Dyrk1a* knockout as described (44,63). Four types of mice from this breeding scheme were analyzed: Ts65Dn ($n=8$), Ts65Dn,$Dyrk1a^{+/-}$ ($n=13$), euploid ($n=14$) and euploid,$Dyrk1a^{+/-}$ ($n=7$). At the age of 6 weeks, multiple skulls/heads from these offspring were imaged at the same time using high resolution micro-computed tomography (μCT; 35 μm resolution) at the Indiana University School of Medicine. The images were segmented into separate heads and 3D bony isosurfaces of μCT image data were visualized and measured using Dolphin software (v11.5; Chatsworth, CA). Anatomical landmark coordinates from the craniofacial skeleton ($n=44$) were identified (Supplementary Material, Fig. S7) and their x, y and z coordinates recorded for morphometric analysis. Additionally, nasopharynx airway volumes (mm^3) were measured from μCT images using Dolphin software (Supplementary Material, Fig. S8). Anatomical landmark coordinate values and nasopharynx airway volumes were measured on two separate occasions with at least 24 h in between measurement sessions

to avoid memory bias, inspected for gross errors and then averaged to minimize potential effects of measurement error.

Differences in skull form among samples were analyzed using 3D landmark coordinate data and Euclidean distance matrix analysis (EDMA) as previously reported (52). EDMA converts 3D landmark coordinate data into an equivalent description of form called a form matrix, which consists of all unique linear distances among landmarks. Morphological differences between samples were statistically compared using a nonparametric bootstrap (10 000 resamples) and confidence interval testing ($\alpha = 0.10$) to determine local differences in craniofacial form. The null hypothesis was that average linear distance measures between the samples are the same (41,42). The percentage of significant differences in summary statistics was calculated by counting the number of significant linear distances in a particular craniofacial region (e.g. cranial vault, face, base or mandible) and dividing it by the total number of unique linear distances for that particular region [i.e. the number of linear distances that could have potentially been significantly different, which is calculated using $\frac{n(n-1)}{n}$, where n is equal to the number of landmarks measured in the region of interest] (44) to assess global region by region differences in patterns of variation across multiple two-sample EDMA form comparisons (4,52). Nasopharyngeal airway volumetric values were compared between samples using independent t-tests.

Supplementary Material

Supplementary Material is available at *HMG* online.

Acknowledgements

We thank Dr Mariona Arbones for providing the *Dyrk1a*$^{+/-}$ mice. We are grateful to Emily Haley and Mariyamou Diallo for help with the embryonic mouse work.

Conflict of Interest statement. None declared.

Funding

National Institutes of Health (DE021034 to R.J.R.), The Indiana Clinical and Translational Sciences Institute funded, in part by Grant Number UL1TR001108 from the National Institutes of Health, National Center for Advancing Translational Sciences, TRAC1 PDT Pilot Grant Mechanism (R.J.R. and S.D.M.), the IUPUI 3D Imaging of the Craniofacial Complex Center (R.J.R., J.M.S., A.G. and K.K.) and National Science Foundation (DSE GK-12 Grant 0742475 to S.D.M. and D.M.T.).

References

1. Borenstein, M., Persico, N., Kaihura, C., Sonek, J. and Nicolaides, K.H. (2007) Frontomaxillary facial angle in chromosomally normal fetuses at 11 + 0 to 13 + 6 weeks. *Ultrasound Obstet. Gynecol.*, **30**, 737–741.
2. Cicero, S., Curcio, P., Rembouskos, G., Sonek, J. and Nicolaides, K.H. (2004) Maxillary length at 11–14 weeks of gestation in fetuses with trisomy 21. *Ultrasound Obstet. Gynecol.*, **24**, 19–22.
3. Sonek, J., Borenstein, M., Dagklis, T., Persico, N. and Nicolaides, K.H. (2007) Frontomaxillary facial angle in fetuses with trisomy 21 at 11–13(6) weeks. *Am. J. Obstet. Gynecol.*, **196**, 271.e1–271.e4.
4. Starbuck, J.M., Cole, T.M., 3rd, Reeves, R.H. and Richtsmeier, J.T. (2013) Trisomy 21 and facial developmental instability. *Am. J. Phys. Anthropol.*, **151**, 49–57.
5. Allanson, J.E., O'Hara, P., Farkas, L.G. and Nair, R.C. (1993) Anthropometric craniofacial pattern profiles in Down syndrome. *Am. J. Med. Genet.*, **47**, 748–752.
6. Fischer-Brandies, H., Schmid, R.G. and Fischer-Brandies, E. (1986) Craniofacial development in patients with Down's syndrome from birth to 14 years of age. *Eur. J. Orthod.*, **8**, 35–42.
7. Richtsmeier, J.T., Baxter, L.L. and Reeves, R.H. (2000) Parallels of craniofacial maldevelopment in Down syndrome and Ts65Dn mice. *Dev. Dyn.*, **217**, 137–145.
8. Starbuck, J., Reeves, R.H. and Richtsmeier, J. (2011) Morphological integration of soft-tissue facial morphology in Down syndrome and siblings. *Am. J. Phys. Anthropol.*, **146**, 560–568.
9. Faulks, D., Collado, V., Mazille, M.N., Veyrune, J.L. and Hennequin, M. (2008) Masticatory dysfunction in persons with Down's syndrome. Part 1: aetiology and incidence. *J. Oral Rehabil.*, **35**, 854–862.
10. Hennequin, M., Faulks, D., Veyrune, J.L. and Bourdiol, P. (1999) Significance of oral health in persons with Down syndrome: a literature review. *Dev. Med. Child Neurol.*, **41**, 275–283.
11. Shott, S.R. (2006) Down syndrome: common otolaryngologic manifestations. *Am. J. Med. Genet. C Semin. Med. Genet.*, **142**, 131–140.
12. Blazek, J.D., Gaddy, A., Meyer, R., Roper, R.J. and Li, J. (2011) Disruption of bone development and homeostasis by trisomy in Ts65Dn Down syndrome mice. *Bone*, **48**, 275–280.
13. Reeves, R.H., Irving, N.G., Moran, T.H., Wohn, A., Kitt, C., Sisodia, S.S., Schmidt, C., Bronson, R.T. and Davisson, M.T. (1995) A mouse model for Down syndrome exhibits learning and behaviour deficits. *Nat. Genet.*, **11**, 177–184.
14. Hill, C.A., Reeves, R.H. and Richtsmeier, J.T. (2007) Effects of aneuploidy on skull growth in a mouse model of Down syndrome. *J. Anat.*, **210**, 394–405.
15. Santagati, F. and Rijli, F.M. (2003) Cranial neural crest and the building of the vertebrate head. *Nat. Rev. Neurosci.*, **4**, 806–818.
16. Helms, J.A. and Schneider, R.A. (2003) Cranial skeletal biology. *Nature*, **423**, 326–331.
17. Knight, R.D. and Schilling, T.F. (2006) Cranial neural crest and development of the head skeleton. *Adv. Exp. Med. Biol.*, **589**, 120–133.
18. Roper, R.J., VanHorn, J.F., Cain, C.C. and Reeves, R.H. (2009) A neural crest deficit in Down syndrome mice is associated with deficient mitotic response to Sonic hedgehog. *Mech. Dev.*, **126**, 212–219.
19. Billingsley, C.N., Allen, J.R., Baumann, D.D., Deitz, S.L., Blazek, J.D., Newbauer, A., Darrah, A., Long, B.C., Young, B., Clement, M. *et al.* (2013) Non-trisomic homeobox gene expression during craniofacial development in the Ts65Dn mouse model of Down syndrome. *Am. J. Med. Genet. A*, **161A**, 1866–1874.
20. Arron, J.R., Winslow, M.M., Polleri, A., Chang, C.P., Wu, H., Gao, X., Neilson, J.R., Chen, L., Heit, J.J., Kim, S.K. *et al.* (2006) NFAT dysregulation by increased dosage of DSCR1 and DYRK1A on chromosome 21. *Nature*, **441**, 595–600.
21. Branchi, I., Bichler, Z., Minghetti, L., Delabar, J.M., Malchiodi-Albedi, F., Gonzalez, M.C., Chettouh, Z., Nicolini, A., Chabert, C., Smith, D.J. *et al.* (2004) Transgenic mouse in vivo library of human Down syndrome critical region 1: association

between DYRK1A overexpression, brain development abnormalities, and cell cycle protein alteration. *J. Neuropathol. Exp. Neurol.*, **63**, 429–440.
22. Canzonetta, C., Mulligan, C., Deutsch, S., Ruf, S., O'Doherty, A., Lyle, R., Borel, C., Lin-Marq, N., Delom, F., Groet, J. *et al.* (2008) DYRK1A-dosage imbalance perturbs NRSF/REST levels, deregulating pluripotency and embryonic stem cell fate in Down syndrome. *Am. J. Hum. Genet.*, **83**, 388–400.
23. Hammerle, B., Ulin, E., Guimera, J., Becker, W., Guillemot, F. and Tejedor, F.J. (2011) Transient expression of Mnb/Dyrk1a couples cell cycle exit and differentiation of neuronal precursors by inducing p27KIP1 expression and suppressing NOTCH signaling. *Development*, **138**, 2543–2554.
24. Yabut, O., Domogauer, J. and D'Arcangelo, G. (2010) Dyrk1A overexpression inhibits proliferation and induces premature neuronal differentiation of neural progenitor cells. *J. Neurosci.*, **30**, 4004–4014.
25. Ahn, K.J., Jeong, H.K., Choi, H.S., Ryoo, S.R., Kim, Y.J., Goo, J.S., Choi, S.Y., Han, J.S., Ha, I. and Song, W.J. (2006) DYRK1A BAC transgenic mice show altered synaptic plasticity with learning and memory defects. *Neurobiol. Dis.*, **22**, 463–472.
26. Altafaj, X., Dierssen, M., Baamonde, C., Marti, E., Visa, J., Guimera, J., Oset, M., Gonzalez, J.R., Florez, J., Fillat, C. *et al.* (2001) Neurodevelopmental delay, motor abnormalities and cognitive deficits in transgenic mice overexpressing Dyrk1A (minibrain), a murine model of Down's syndrome. *Hum. Mol. Genet.*, **10**, 1915–1923.
27. Martinez de Lagran, M., Altafaj, X., Gallego, X., Marti, E., Estivill, X., Sahun, I., Fillat, C. and Dierssen, M. (2004) Motor phenotypic alterations in TgDyrk1a transgenic mice implicate DYRK1A in Down syndrome motor dysfunction. *Neurobiol. Dis.*, **15**, 132–142.
28. Lee, Y., Ha, J., Kim, H.J., Kim, Y.S., Chang, E.J., Song, W.J. and Kim, H.H. (2009) Negative feedback inhibition of NFATc1 by DYRK1A regulates bone homeostasis. *J. Biol. Chem.*, **284**, 33343–33351.
29. Blazek, J.D., Abeysekera, I., Li, J. and Roper, R.J. (2015) Rescue of the abnormal skeletal phenotype in Ts65Dn Down syndrome mice using genetic and therapeutic modulation of trisomic Dyrk1a. *Hum. Mol. Genet.*, **24**, 5687–5696.
30. Becker, W., Soppa, U. and Tejedor, F.J. (2014) DYRK1A: a potential drug target for multiple Down syndrome neuropathologies. *CNS Neurol. Disord. Drug Targets*, **13**, 26–33.
31. Chu, K.O., Wang, C.C., Chu, C.Y., Choy, K.W., Pang, C.P. and Rogers, M.S. (2007) Uptake and distribution of catechins in fetal organs following in utero exposure in rats. *Hum. Reprod.*, **22**, 280–287.
32. Guedj, F., Sebrie, C., Rivals, I., Ledru, A., Paly, E., Bizot, J.C., Smith, D., Rubin, E., Gillet, B., Arbones, M. *et al.* (2009) Green tea polyphenols rescue of brain defects induced by overexpression of DYRK1A. *PLoS One*, **4**, e4606.
33. De la Torre, R., De Sola, S., Pons, M., Duchon, A., de Lagran, M.M., Farre, M., Fito, M., Benejam, B., Langohr, K., Rodriguez, J. *et al.* (2014) Epigallocatechin-3-gallate, a DYRK1A inhibitor, rescues cognitive deficits in Down syndrome mouse models and in humans. *Mol. Nutr. Food Res.*, **58**, 278–288.
34. De la Torre, R., de Sola, S., Hernandez, G., Farre, M., Pujol, J., Rodriguez, J., Espadaler, J.M., Langohr, K., Cuenca-Royo, A., Principe, A. *et al.* (2016) Safety and efficacy of cognitive training plus epigallocatechin-3-gallate in young adults with Down's syndrome (TESDAD): a double-blind, randomised, placebo-controlled, phase 2 trial. *Lancet. Neurol.*, **15**, 801–810.
35. Stagni, F., Giacomini, A., Emili, M., Trazzi, S., Guidi, S., Sassi, M., Ciani, E., Rimondini, R. and Bartesaghi, R. (2016) Short- and long-term effects of neonatal pharmacotherapy with epigallocatechin-3-gallate on hippocampal development in the Ts65dn mouse model of Down syndrome. *Neuroscience*, **333**, 277–301.
36. Ranger, A.M., Gerstenfeld, L.C., Wang, J., Kon, T., Bae, H., Gravallese, E.M., Glimcher, M.J. and Glimcher, L.H. (2000) The nuclear factor of activated T cells (NFAT) transcription factor NFATp (NFATc2) is a repressor of chondrogenesis. *J. Exp. Med.*, **191**, 9–22.
37. Adayev, T., Wegiel, J. and Hwang, Y.W. (2011) Harmine is an ATP-competitive inhibitor for dual-specificity tyrosine phosphorylation-regulated kinase 1A (Dyrk1A). *Arch. Biochem. Biophys.*, **507**, 212–218.
38. Hill, C.A., Sussan, T.E., Reeves, R.H. and Richtsmeier, J.T. (2009) Complex contributions of Ets2 to craniofacial and thymus phenotypes of trisomic "Down syndrome" mice. *Am. J. Med. Genet. A*, **149A**, 2158–2165.
39. Singh, N., Dutka, T., Devenney, B.M., Kawasaki, K., Reeves, R.H. and Richtsmeier, J.T. (2015) Acute upregulation of hedgehog signaling in mice causes differential effects on cranial morphology. *Dis. Model Mech.*, **8**, 271–279.
40. Stringer, M., Abeysekera, I., Dria, K.J., Roper, R.J. and Goodlett, C.R. (2015) Low dose EGCG treatment beginning in adolescence does not improve cognitive impairment in a Down syndrome mouse model. *Pharm. Biochem. Behav.*, **138**, 70–79.
41. Lele, S. and Richtsmeier, J.T. (1991) Euclidean distance matrix analysis: a coordinate-free approach for comparing biological shapes using landmark data. *Am. J. Phys. Anthropol.*, **86**, 415–427.
42. Lele, S. and Richtsmeier, J.T. (2001) *An Invariant Approach to Statistical Analysis of Shapes*. Chapman and Hall-CRC Press, London.
43. Roper, R.J., St John, H.K., Philip, J., Lawler, A. and Reeves, R.H. (2006) Perinatal loss of Ts65Dn Down syndrome mice. *Genetics*, **172**, 437–443.
44. Fotaki, V., Dierssen, M., Alcantara, S., Martinez, S., Marti, E., Casas, C., Visa, J., Soriano, E., Estivill, X. and Arbones, M.L. (2002) Dyrk1A haploinsufficiency affects viability and causes developmental delay and abnormal brain morphology in mice. *Mol. Cell Biol.*, **22**, 6636–6647.
45. Solzak, J.P., Liang, Y., Zhou, F.C. and Roper, R.J. (2013) Commonality in Down and fetal alcohol syndromes. *Birth Defects Res. A Clin. Mol. Teratol.*, **97**, 187–197.
46. Blazek, J.D., Malik, A.M., Tischbein, M., Arbones, M.L., Moore, C.S. and Roper, R.J. (2015) Abnormal mineralization of the Ts65Dn Down syndrome mouse appendicular skeleton begins during embryonic development in a Dyrk1a-independent manner. *Mech. Dev.*, **136**, 133–142.
47. Bain, J., McLauchlan, H., Elliott, M. and Cohen, P. (2003) The specificities of protein kinase inhibitors: an update. *Biochem. J.*, **371**, 199–204.
48. Currier, D.G., Polk, R.C. and Reeves, R.H. (2012) A Sonic hedgehog (Shh) response deficit in trisomic cells may be a common denominator for multiple features of Down syndrome. *Prog. Brain Res.*, **197**, 223–236.
49. Mao, J., Maye, P., Kogerman, P., Tejedor, F.J., Toftgard, R., Xie, W., Wu, G.,. and Wu, D. (2002) Regulation of Gli1 transcriptional activity in the nucleus by Dyrk1. *J. Biol. Chem.*, **277**, 35156–35161.
50. Morita, K., Lo Celso, C., Spencer-Dene, B., Zouboulis, C.C. and Watt, F.M. (2006) HAN11 binds mDia1 and controls GLI1 transcriptional activity. *J. Dermatol. Sci.*, **44**, 11–20.

51. Wang, Y., Li, M., Xu, X., Song, M., Tao, H. and Bai, Y. (2012) Green tea epigallocatechin-3-gallate (EGCG) promotes neural progenitor cell proliferation and sonic hedgehog pathway activation during adult hippocampal neurogenesis. *Mol. Nutr. Food Res.*, **56**, 1292–1303.
52. Starbuck, J.M., Dutka, T., Ratliff, T.S., Reeves, R.H. and Richtsmeier, J.T. (2014) Overlapping trisomies for human chromosome 21 orthologs produce similar effects on skull and brain morphology of Dp(16)1Yey and Ts65Dn mice. *Am. J. Med. Genet. A*, **164A**, 1981–1990.
53. Fotaki, V., Martinez De Lagran, M., Estivill, X., Arbones, M. and Dierssen, M. (2004) Haploinsufficiency of Dyrk1A in mice leads to specific alterations in the development and regulation of motor activity. *Behav. Neurosci.*, **118**, 815–821.
54. Roper, R.J. and Reeves, R.H. (2006) Understanding the basis for Down syndrome phenotypes. *PLoS Genet.*, **2**, e50.
55. Le Douarin, N.M., Brito, J.M. and Creuzet, S. (2007) Role of the neural crest in face and brain development. *Brain Res. Rev.*, **55**, 237–247.
56. Le Douarin, N.M. and Dupin, E. (2012) The neural crest in vertebrate evolution. *Curr. Opin. Genet. Dev.*, **22**, 381–389.
57. Richtsmeier, J.T. and Flaherty, K. (2013) Hand in glove: brain and skull in development and dysmorphogenesis. *Acta Neuropathol.*, **125**, 469–489.
58. Blazek, J.D., Billingsley, C.N., Newbauer, A. and Roper, R.J. (2010) Embryonic and not maternal trisomy causes developmental attenuation in the Ts65Dn mouse model for Down syndrome. *Dev. Dyn.*, **239**, 1645–1653.
59. Dutka, T., Hallberg, D. and Reeves, R.H. (2015) Chronic up-regulation of the SHH pathway normalizes some developmental effects of trisomy in Ts65Dn mice. *Mech. Dev.*, **135**, 68–80.
60. Singh, N., Dutka, T., Reeves, R.H. and Richtsmeier, J.T. (2016) Chronic up-regulation of sonic hedgehog has little effect on postnatal craniofacial morphology of euploid and trisomic mice. *Dev. Dyn.*, **245**, 114–122.
61. Guedj, F. and Bianchi, D.W. (2013) Noninvasive prenatal testing creates an opportunity for antenatal treatment of Down syndrome. *Prenat. Diagn.*, **33**, 614–618.
62. Stagni, F., Giacomini, A., Guidi, S., Ciani, E. and Bartesaghi, R. (2015) Timing of therapies for Down syndrome: the sooner, the better. *Front. Behav. Neurosci.*, **9**, 265.
63. Reinholdt, L.G., Ding, Y., Gilbert, G.J., Czechanski, A., Solzak, J.P., Roper, R.J., Johnson, M.T., Donahue, L.R., Lutz, C. and Davisson, M.T. (2011) Molecular characterization of the translocation breakpoints in the Down syndrome mouse model Ts65Dn. *Mamm. Genome*, **22**, 685–691.
64. Moore, C.S., Lee, J.S., Birren, B., Stetten, G., Baxter, L.L. and Reeves, R.H. (1999) Integration of cytogenetic with recombinational and physical maps of mouse chromosome 16. *Genomics*, **59**, 1–5.
65. Dunn, K.W., Kamocka, M.M. and McDonald, J.H. (2011) A practical guide to evaluating colocalization in biological microscopy. *Am. J. Physiol. Cell Physiol*, **300**, C723–C742.
66. Zhao, H., Bringas, P., Jr. and Chai, Y. (2006) An in vitro model for characterizing the post-migratory cranial neural crest cells of the first branchial arch. *Dev. Dyn.*, **235**, 1433–1440.
67. Liang, C.C., Park, A.Y. and Guan, J.L. (2007) In vitro scratch assay: a convenient and inexpensive method for analysis of cell migration in vitro. *Nat. Protoc.*, **2**, 329–333.
68. Pfaffl, M.W. (2001) A new mathematical model for relative quantification in real-time RT-PCR. *Nucleic Acids Res.*, **29**, e45.
69. Long, L., Li, Y., Wang, Y.D., He, Q.Y., Li, M., Cai, X.D., Peng, K., Li, X.P., Xie, D., Wen, Y.L. *et al.* (2010) The preventive effect of oral EGCG in a fetal alcohol spectrum disorder mouse model. *Alcohol Clin. Exp. Res.*, **34**, 1929–1936.
70. Mouton, P.R. (2002) *Principles and Practices of Unbiased Stereology: An Introduction for Bioscientists*. Johns Hopkins University Press, Baltimore.